ChemComm

COMMUNICATION

View Article Online
View Journal | View Issue

Cite this: *Chem. Commun.*, 2021, 57, 5965

Received 12th April 2021,
Accepted 13th May 2021

DOI: 10.1039/d1cc01939b

rsc.li/chemcomm

Distinctly different reactivity of bis(silylenyl)- *versus* phosphanyl-silylenyl-substituted *o*-dicarborane towards O_2, N_2O and CO_2†

Yun Xiong, [a] Shenglai Yao, [a] Ales Ruzicka [b] and Matthias Driess *[a]

In stark contrast to the reactivity of the bis-silylenyl dicarborane CB–Si_2 (1) [CB = *ortho*-*C*,*C*′-$C_2B_{10}H_{10}$, Si = PhC(*t*BuN)$_2$Si] towards O_2, N_2O, and CO_2, yielding the same dioxygenation product CB–Si_2O_2 (2) with a four-membered 1,3,2,4-disiladioxetane ring, the activation of the latter small molecules with the phosphanyl-silylenyl-functionalised CB–SiP (3) {P═P[N(*t*Bu)CH_2]$_2$} affords with O_2 the CB–Si(═O)P(═O) silanone-phosphine oxide (4), with N_2O the CB–Si(═O)P silanone-phosphine (5), and with CO_2 the CB–Si(O_2C═O)P silicon carbonate-phosphine (6) and CB–C(═O)OSiOP ester (7), respectively.

For many decades, the activation of ubiquitous small molecules such as H_2, N_2, O_2, CO, CO_2, N_2O, *etc.* has been considered to be a domain of transition-metal chemistry and metalloenzymes, including their low molecular-weight functional models. However, recent advances in low-valent non- and semi-metal chemistry have provided a plethora of impressive evidence with transition-metal-like reactivity of main-group elements in small molecule activation.[1–6] This is in part due to the availability of reactive lone pair electrons and relatively low-lying empty acceptor orbitals of main-group elements in unusual low oxidation states, which can mimic the electronic situation of transition-metal centres and even mediate chemical bond cleavage of unactivated small molecules. Striking examples comprise the activation of dihydrogen by acyclic silylenes with a highly reactive silicon(II) centre[7–10] and the fixation of dinitrogen by a borylene as a carbene analogue.[11,12] In recent years, we have been interested in the chemistry of chelating N-heterocyclic silylenes (NHSis) that feature two adjacent divalent silicon atoms as highly reactive sites.[13–15] Such bis-NHSis not only can serve as steering ligands for coordination of main-group elements in unusual low oxidation states and transition metals for catalysis,[13–15] they can also mediate cooperative small molecule activation through sufficiently close proximity of the two silicon(II) centres.[16,17] For instance, the bis-NHSis with a Si···Si distances between 2.6 and 4.5 Å are capable reacting with CO at ambient temperature, affording disilaketenes.[16–18] Featuring a Si···Si distance of about 3.3 Å, the two Si(II) centres in the *ortho*-dicarborane-based bis-NHSi CB–**SiSi** (**1**)[19] (Scheme 1) are in a predestinate position to coordinate and subsequently activate CO.[17] Moreover, the bis-NHSi **1** has been employed to stabilise a single zero-valent Si atom,[20] monovalent boron,[21] and serves in nickel-mediated catalytic transformations.[19] More recently we succeeded in the synthesis of the isolobal phosphanyl-silylenyl-functionalised *o*-dicarborane CB–**SiP** (**3**) where one silylenyl group in **1** is replaced by a phosphanyl moiety.[22] Compound **3** enabled the formation of new classes of *C*,*C*′-dicarborandiyl-silylene supported Ge_2 and Ge_4 species which could not be realised with **1**.[22] Herein, we wish to report the markedly different reactivity of **1** and **3** towards O_2, N_2O, and CO_2, respectively.

Exposure of solutions of **1** in diethyl ether at −20 °C to O_2 gas leads to immediate disappearance of the yellow color and formation of the 1,3,2,4-disiladioxetane **2** (Scheme 1).

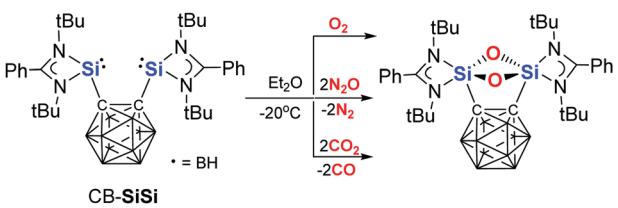

Scheme 1 Reactions of **1** with O_2, N_2O, and CO_2 to yield **2**.

[a] *Metalorganics and Inorganic Materials, Department of Chemistry, Technische Universität Berlin, Straße des 17, Juni 135, Sekr. C2, Berlin 10623, Germany. E-mail: matthias.driess@tu-berlin.de; Web: http://www.driess.tu-berlin.de; Fax: +49-30-314-29732*

[b] *Department of General and Inorganic Chemistry, Faculty of Chemical Technology, University of Pardubice, Studentska 573, 532 10 Pardubice, Czech Republic*

† Electronic supplementary information (ESI) available: Experimental methods, crystallographic details. CCDC 2075598 (compound **2**), 2075596 (compound **4**), 2075600 (compound **5**), 2075599 (compound **6**), and 2075597 (compound **7**). For ESI and crystallographic data in CIF or other electronic format see DOI: 10.1039/d1cc01939b

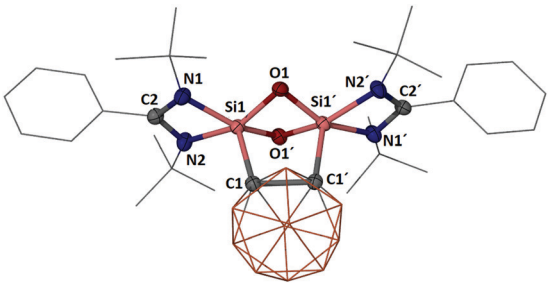

Fig. 1 Molecular structure of **2**. Thermal ellipsoids are drawn at 50% probability level. Hydrogen atoms and one toluene molecule are omitted for clarity. Selected bond distances (Å) and angles (°): Si1–O1 1.695(1), Si1–O1′ 1.708(1), Si1–C1 1.961(2), Si1–N1 1.861(1), Si1–N2 1.884(1), Si1–Si1′ 2.403(1); O1–Si1–O1′ 83.4(1), Si1–O1–Si1′ 89.8(1), O1–Si1–C1 96.6(1), O1′–Si1–C1 96.1(1).

Interestingly, **2** is also formed as single product through exposure of **1** towards N_2O and CO_2 under the same reaction conditions. After workup, **2** has been isolated as a colorless solid; it crystallises in the monoclinic space group *C*2/*c*. The two Si centres are five-coordinated and bridged by two oxygen atoms (Fig. 1). The Si atoms adopt a distorted square-pyramidal coordination geometry with the carborane–C atom at the apical position. The Si1–O1 [1.695(1) Å] and Si1–O1′ [1.708(1) Å] distances in **2** are slightly longer than the Si–O length in octamethyl cyclotetrasiloxane (*ca.* 1.65 Å).[23] As expected, the five-coordinate ^{29}Si nuclei exhibit a drastic up-field shift in the ^{29}Si{^{1}H} NMR spectrum (δ = −98.6 ppm) when compared with the precursor **1** (δ = 18.9 ppm).[19]

The reactions of O_2, N_2O, and CO_2 with various stable silylenes to give Si=O-containing compounds or further oxygenated Si–O-containing species are well-documented.[5,9,24–30] We wondered whether a transient or even isolable Si=O species could be detected if one silylenyl moiety in **1** is replaced by a isoelectronic phosphanyl group; thus we employed the phosphanyl-silylenyl-functionalised carborane CB–**SiP** (**3**). Indeed, under the same reaction conditions, exposure of **3** to dioxygen gas at −20 °C resulted in the formation of the CB–**Si**(=O)**P**(=O) silanone-phosphine oxide (**4**) (Scheme 2 and Fig. 2), in which both P and Si atoms are mono-oxygenated. Compound **4** was isolated at −20 °C as a colorless solid in 68% yields. It is sparingly soluble in Et_2O, but well soluble in THF. Solutions of **4** in ethereal solvents are only stable below −20 °C; its decomposition affords a mixture of unidentified products. In the solid state, however, **4** is stable at room temperature and decomposes above 153 °C.

The ^{31}P{^{1}H} NMR spectrum of **4** (measured at −20 °C in d_8-THF) exhibits a singlet at δ = 26.4 ppm, which is significantly up-field shifted relative to that of the precursor **3** (δ = 102.9 ppm).[22] A similar up-field shift is observed for the ^{29}Si{^{1}H} NMR resonance of **4** (δ = −52.8 *vs.* 17.5 ppm for **3**).[22] The IR spectrum of **4** shows a very strong stretching vibration mode at ν = 1193 cm^{-1} for the Si=O bond, which is slightly larger than the value observed for the Si=O bond in a C=O-supported silanone (1153 cm^{-1}).[27] A single-crystal X-ray diffraction analysis confirmed the presence of Si=O and P=O

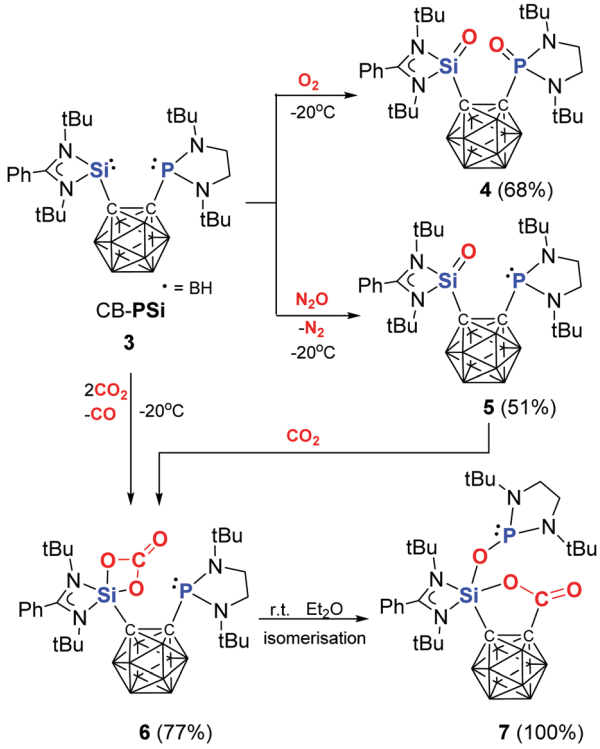

Scheme 2 Reactions of CB-**PSi** 3 with N_2O, O_2, and CO_2 to give 4, 5, 6 and 7.

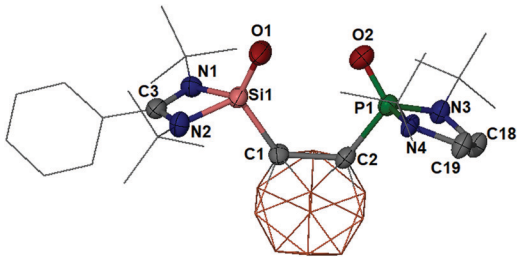

Fig. 2 Molecular structure of **4** (There are two molecules in the asymmetric unit, only one is depicted). Thermal ellipsoids are drawn at 50% probability level. Hydrogen atoms are omitted for clarity. Selected bond distances (Å) and angles (°) for molecule 1: Si1–O1 1.524(3), Si1–C1 1.943(4), Si1–N1 1.820(3), Si1–N2 1.814(3), P1–O2 1.456(3), P1–C2 1.899(4), P1–N3 1.638(3), P1–N4 1.656(3); O1–Si1–C1 122.5(2), O2–P1–C2 109.2(2).

bonds in **4** with a O1–Si1–P1–O2 torsion angle of 36.8° (Fig. 2). In **4** both silicon and phosphorus atoms adopt a distorted tetrahedral coordination environment. In line with the IR spectroscopic data, the Si–O distance of 1.524(3) Å in **4** is slightly shorter than that in the aforementioned keto-supported silanone adduct [1.532(2) Å],[27] indicating a more pronounced Si=O bond character.

As mentioned above, the reaction of silylenes with dioxygen usually affords disiladioxetanes or related Si–O single bond containing products. The formation of **4** as an isolable Si=O species is apparently due to the presence of the phosphanyl

moiety, acting as an oxygen atom acceptor in close proximity to the silicon atom. In order to figure out whether **3** is capable of N_2O activation to furnish a Si=O-(and/or P=O)-containing product, we exposed solutions of **3** in Et_2O to N_2O gas at −20 °C. To our surprise, the oxygenation took place only at the silicon centre to form the CB-(**Si**=O)**P** silanone-phosphine (**5**), which could be isolated in 51% yields (Scheme 2). This is consistent with the fact, that such substituted phosphines are inert toward N_2O. Akin to **4**, compound **5** is labile in Et_2O and THF solutions above −20 °C and decomposes to an unidentified mixture of products. However, **5** is indefinitely stable in the solid state at ambient temperature and decomposes above 176 °C.

The molecular structure of **5** established by a single-crystal X-ray diffraction analysis revealed a four-coordinate silicon atom with a distorted tetrahedral coordination geometry (Fig. 3), while the phosphorus atom remains unchanged with respect to the precursor **3**. The Si=O distance of 1.524(1) Å in **5** is identical to that in **4**. In line with that, the IR spectrum of **5** exhibits a Si=O stretching frequency of 1187 cm^{-1}, which is very close to the value observed for **4** (ν = 1193 cm^{-1}). The four-coordinate Si atom in **5** shows a resonance at δ = −51.9 ppm in the $^{29}Si\{^1H\}$ NMR spectrum (measured at −30 °C in d_8-THF), matching well with that for **4** (δ = −52.8 ppm). In contrast, the marginally different chemical shift at δ = 114.2 ppm in the $^{31}P\{^1H\}$ NMR spectrum of **5** (*vs.* δ = 102.9 ppm of its precursor **3**)[22] confirms the presence of the unchanged phosphine moiety.

As aforementioned, previous studies on CO_2 activation toward silylenes revealed mono-oxygen transfer and liberation of CO to form either Si=O[26,28–30] or dimeric disiladioxetane species.[29,31] in less cases, silicon carbonates[31–34] could be isolated which resulted from trapping reaction of Si=O intermediate with CO_2. Similar to the reactivity of **3** towards N_2O, **3** reacts with CO_2 in diethyl ether at −20 °C only at the Si(II) site to yield the CB-(**Si**O_2C=O)**P** silicon carbonate-phosphine (**6**) (Scheme 2). The latter product was isolated in 77% yields after workup at low temperature. The $^{31}P\{^1H\}$ NMR spectrum of **6** shows a signal at δ = 115.5 ppm (measured at −10 °C in d_8-THF), indicating the presence of the unchanged phosphine moiety, whereas the $^{29}Si\{^1H\}$ NMR spectrum shows a resonance at δ = −93.1 ppm, reminiscent of the five-coordinate ^{29}Si nuclei attached to a ferrocene spacer (δ = −92.1 ppm).[29] The IR spectrum of **6** exhibits a stretching vibration mode at ν = 1813 cm^{-1} for the C=O group, comparable to that observed in a bis-NHC-supported silicon dicarbonate (1746 cm^{-1}).[35] A single-crystal X-ray diffraction analysis confirmed the molecular structure of **6** (Fig. 4), which features a five-coordinate silicon atom in a strongly distorted square-pyramidal coordination geometry with the carborane–C atom at the apical position. The Si–O distances of 1.718(1) and 1.770(1) Å in **6** are significantly longer than the Si=O lengths in **4** and **5**, respectively, but close to the Si–O bonds in **2** [1.695(1), 1.708(1) Å]. The C3–O1 distance of 1.194(2) Å is considerably shorter than those of C3–O2 (1.362(2) Å) and C3–O3 (1.340(2) Å), implying a C=O bond between C3 and O1.

Although the mechanism of **6** from **3** with CO_2 is still unknown, we propose that the initial step of the reaction is the formation of **5** with a Si=O moiety under release of CO. To prove this, we conducted the reaction of **5**, obtained from **3** and N_2O, with CO_2 at −20 °C (Scheme 2). Indeed, a clean formation of **6** confirmed this by multinuclear NMR spectroscopy measurements.

While **6** is stable at room temperature in the solid state, it isomerises quantitatively at room temperature in ethereal solvents to give **7** in the course of 24 hours (Scheme 2). Its molecular structure has been established by a single-crystal X-ray diffraction analysis. As depicted in Fig. 5, the silicon atom in **7** is five-coordinate and in a distorted trigonal-bipyramidal coordination environment with the N1 and O2 atoms in the axial positions. Thus, the Si1–O2 distance of 1.773(2) Å is longer than that of Si1–O3 (1.624(2) Å). The driving force of the isomerization of **6** to **7** is attributed to the oxygen affinity of phosphorus that induces CB C–P bond scission and CB C–CO bond formation. In addition, the steric congestion in **6** between the phosphine group and the CB cage is released after migration of the phosphine moiety from the carborane-C2 to the

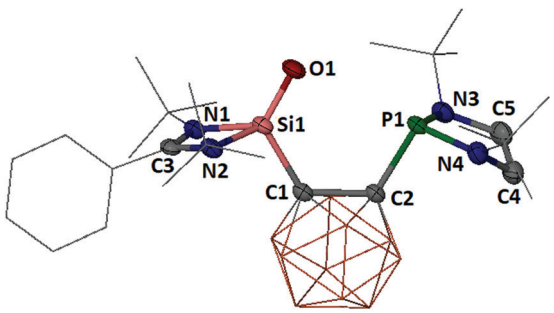

Fig. 3 Molecular structure of **5**. Thermal ellipsoids are drawn at 50% probability level. Hydrogen atoms are omitted for clarity. Selected bond distances (Å) and angles (°): Si1–O1 1.524(1), Si1–C1 1.930(2), Si1–N1 1.827(2), Si1–N2 1.814(2), P1–C2 1.949(1), P1–N3 1.717(2), P1–N4 1.677(2); O1–Si1–C1 120.2(1).

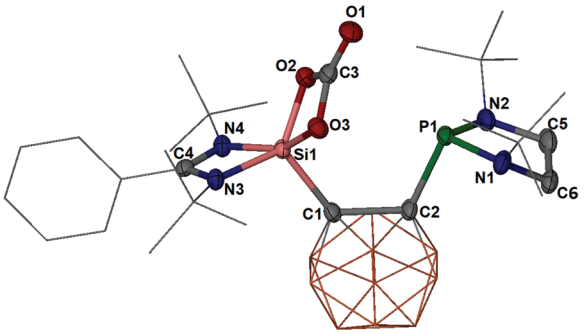

Fig. 4 Molecular structure of **6**. Thermal ellipsoids are drawn at 50% probability level. Hydrogen atoms are omitted for clarity. Selected bond distances (Å) and angles (°): Si1–O2 1.718(1), Si1–O3 1.770(1), Si1–C1 1.939(2), Si1–N3 1.811(2), Si1–N4 1.874(2), P1–C2 1.932(2), P1–N1 1.684(2), P1–N2 1.708(2), C3–O1 1.194(2), C3–O2 1.362(2), C3–O3 1.340(2), C1–C2 1.738(3); O2–Si1–C1 117.5(1), O3–Si1–C1 102.1(1), N3–Si1–C1 109.8(1), N4–Si1–C1 103.2(1), O2–Si1–O3 75.0(1), O1–C3–O2 126.9(2), O1–C3–O3 129.3(2), O2–C3–O3 103.7(2).

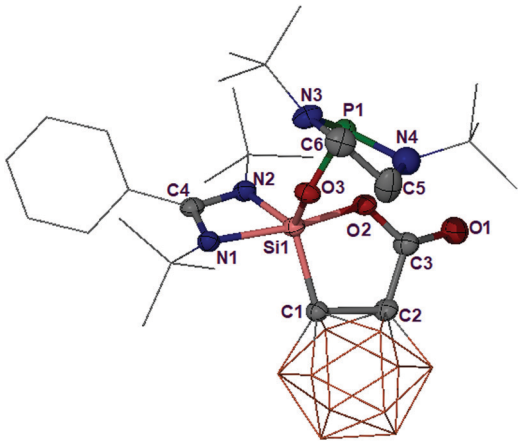

Fig. 5 Molecular structure of **7**. Thermal ellipsoids are drawn at 50% probability level. Hydrogen atoms are omitted for clarity. Selected bond distances (Å) and angles (°): Si1–O2 1.773(2), Si1–O3 1.624(2), Si1–C1 1.937(3), O3–P1 1.666(2), O2–C3 1.314(3), O1–C3 1.200(3), C2–C3 1.515(4), C1–C2 1.652(3); O3–Si1–O2 94.2(1), O3–Si1–N2 120.2(1), N2–Si1–C1 118.3(1), O3–Si1–C1 120.6(1), N1–Si1–O2 167.8(1), Si1–O3–P1 134.7(1), O2–C3–O1 125.5(2), O1–C3–C2 122.4(2), O2–C3–C2 112.1(2).

O3 atom. As a result, the C1–C2 distance of 1.652(3) Å in **7** is significantly shorter than that in **6** (1.738(3) Å). In accordance with the molecular structure of **7**, its $^{29}Si\{^{1}H\}$ NMR spectrum shows a doublet at $\delta = -110.4$ ppm ($^{2}J_{(Si,P)} = 9.4$ Hz) comparable to that of **6** ($\delta = -93.1$ ppm), and the ^{31}P nucleus resonates at $\delta = 119.6$ ppm in the $^{31}P\{^{1}H\}$ NMR spectrum reminiscent of that for **6** ($\delta = 115.5$ ppm).

In summary, we have described the markedly different reactivity of the bis-NHSi dicarborane **1** and its isolobal phosphanyl-NHSi-functionalised dicarborane analogue **3** towards O_2, N_2O, and CO_2. While all reactions of **1** with O_2, N_2O, and CO_2 let to the same dioxygenation product CB–**Si**(μ-O)$_2$**Si** **2**, the activation products with **3** turned out to furnish different products featuring Si═O, P═O, or C═O functionalities.

Financial support by the Deutsche Forschungsgemeinschaft (Germany's Excellence Strategy–EXC 2008–390540038–UniSysCat and DR 226/21-1) and the Czech Science Foundation (A. R., project no. 21-02964S) is gratefully acknowledged.

Conflicts of interest

There are no conflicts to declare.

Notes and references

1 P. P. Power, *Nature*, 2010, **463**, 171–177.
2 T. Chu and G. I. Nikonov, *Chem. Rev.*, 2018, **118**, 3608–3680.
3 S. Yadav, S. Saha and S. S. Sen, *ChemCatChem*, 2016, **8**, 486–501.
4 C. Weetman and S. Inoue, *ChemCatChem*, 2018, **10**, 4213–4228.
5 C. Shan, S. Yao and M. Driess, *Chem. Soc. Rev.*, 2020, **49**, 6733–6754.
6 R. L. Melen, *Science*, 2019, **363**, 479–484.
7 A. V. Protchenko, K. H. Birjkumar, D. Dange, A. D. Schwarz, D. Vidovic, C. Jones, N. Kaltsoyannis, P. Mountford and S. Aldridge, *J. Am. Chem. Soc.*, 2012, **134**, 6500–6503.
8 A. V. Protchenko, A. D. Schwarz, M. P. Blake, C. Jones, N. Kaltsoyannis, P. Mountford and S. Aldridge, *Angew. Chem., Int. Ed.*, 2013, **52**, 568–571.
9 D. Reiter, R. Holzner, A. Porzelt, P. J. Altmann, P. Frisch and S. Inoue, *J. Am. Chem. Soc.*, 2019, **141**, 13536–13546.
10 S. Takahashi, E. Bellan, A. Baceiredo, N. Saffon-Merceron, S. Massou, N. Nakata, D. Hashizume, V. Branchadell and T. Kato, *Angew. Chem., Int. Ed.*, 2019, **58**, 10310–10314.
11 M.-A. Legare, G. Belanger-Chabot, R. D. Dewhurst, E. Welz, I. Krummenacher, B. Engels and H. Braunschweig, *Science*, 2018, **359**, 896–900.
12 M.-A. Legare, M. Rang, G. Belanger-Chabot, J. I. Schweizer, I. Krummenacher, R. Bertermann, M. Arrowsmith, M. C. Holthausen and H. Braunschweig, *Science*, 2019, **1332**, 1329–1332.
13 Y.-P. Zhou and M. Driess, *Angew. Chem., Int. Ed.*, 2019, **58**, 3715–3728.
14 S. Raoufmoghaddam, Y. P. Zhou, Y. Wang and M. Driess, *J. Organomet. Chem.*, 2017, **829**, 2–10.
15 B. Blom, D. Gallego and M. Driess, *Inorg. Chem. Front.*, 2014, **1**, 134–148.
16 Y. Wang, A. Kostenko, T. J. Hadlington, M.-P. Luecke, S. Yao and M. Driess, *J. Am. Chem. Soc.*, 2019, **141**, 626–634.
17 Y. Xiong, S. Yao, T. Szilva, A. Ruzicka and M. Driess, *Chem. Commun.*, 2020, **56**, 747–750.
18 A. Kostenko and M. Driess, *J. Am. Chem. Soc.*, 2018, **140**, 16962–16966.
19 Y.-P. Zhou, S. Raoufmoghaddam, T. Szilvási and M. Driess, *Angew. Chem., Int. Ed.*, 2016, **55**, 12868–12872.
20 S. Yao, A. Kostenko, Y. Xiong, A. Ruzicka and M. Driess, *J. Am. Chem. Soc.*, 2020, **142**, 12608–12612.
21 H. Wang, L. Wu, Z. Lin and Z. Xie, *J. Am. Chem. Soc.*, 2017, **139**, 13680–13683.
22 Y. Xiong, D. Chen, S. Yao, J. Zhu, A. Ruzicka and M. Driess, *J. Am. Chem. Soc.*, 2021, **143**, 6229–6237.
23 H. Steinfink, B. Post and I. Fankuchen, *Acta Crystallogr.*, 1955, **8**, 420–424.
24 M. Asay, C. Jones and M. Driess, *Chem. Rev.*, 2011, **111**, 354–396.
25 (*a*) R. Rodriguez, T. Troadec, D. Gau, N. Saffon-Merceron, D. Hashizume, K. Miqueu, J.-M. Sotiropoulos, A. Baceiredo and T. Kato, *Angew. Chem.*, 2013, **52**, 4426–4430; (*b*) A. C. Filippou, B. Baars, O. Chernov, Y. N. Lebedev and G. Schnakenburg, *Angew. Chem., Int. Ed.*, 2014, **53**, 565–570; (*c*) D. C. H. Do, A. V. Protchenko, M. Angeles Fuentes, J. Hicks, E. L. Kolychev, P. Vasko and S. Aldridge, *Angew. Chem., Int. Ed.*, 2018, **57**, 13907–13911; (*d*) R. Kobayashi, S. Ishida and T. Iwamoto, *Angew. Chem., Int. Ed.*, 2019, **58**, 9425–9428; (*e*) S. Takahashi, K. Nakaya, M. Frutos, A. Baceiredo, N. Saffon-Merceron, S. Massou, N. Nakata, D. Hashizume, V. Branchadell and T. Kato, *Angew. Chem., Int. Ed.*, 2020, **59**, 15937–15941.
26 S. Yao, Y. Xiong, M. Brym and M. Driess, *J. Am. Chem. Soc.*, 2007, **129**, 7268–7269.
27 Y. Xiong, S. Yao, R. Müller, M. Kaupp and M. Driess, *Nat. Chem.*, 2010, **2**, 577–580.
28 S. U. Ahmad, T. Szilvási, E. Irran and S. Inoue, *J. Am. Chem. Soc.*, 2015, **137**, 5828–5836.
29 M. P. Luecke, E. Pens, S. Yao and M. Driess, *Chem. – Eur. J.*, 2020, **26**, 4500–4504.
30 Z. Mo, T. Szilvási, Y. P. Zhou, S. Yao and M. Driess, *Angew. Chem., Int. Ed.*, 2017, **56**, 3699–3702.
31 F. M. Mück, J. A. Baus, M. Nutz, C. Burschka, J. Poater, F. M. Bickelhaupt and R. Tacke, *Chem. – Eur. J.*, 2015, **21**, 16665–16672.
32 D. Wendel, A. Porzelt, F. A. D. Herz, D. Sarkar, C. Jandl, S. Inoue and B. Rieger, *J. Am. Chem. Soc.*, 2017, **139**, 8134–8137.
33 P. Jutzi, D. Eikenberg, A. Möhrke, B. Neumann and H. G. Stammler, *Organometallics*, 1996, **15**, 753–759.
34 C. Yan, Z. Xu, X. Q. Xiao, Z. Li, Q. Lu, G. Lai and M. Kira, *Organometallics*, 2016, **35**, 1323–1328.
35 A. Burchert, S. Yao, R. Müller, C. Schattenberg, Y. Xiong, M. Kaupp and M. Driess, *Angew. Chem., Int. Ed.*, 2017, **56**, 1894–1897.

